geosciences

MDPI

Article

Should Anthropic Ridges Framed as Foredunes Be Considered Real Dunes?

Alexandre Medeiros de Carvalho [1], Vanda Claudino-Sales [2,*], Sergio Bezerra Lima Junior [1], Leticia Mesquita Eduardo [1], Francisco Gleidson da Costa Gastão [1] and Lidriana de Souza Pinheiro [1,3]

[1] Instituto de Ciências do Mar-LABOMAR, Universidade Federal do Ceará, Fortaleza 60165-081, Brazil
[2] Department of Geography Federal University of Ceará, Universidade do Vale do Acaraú (UVA), Sobral 62040-370, Brazil
[3] Dipartimento di Scienze e Tecnologie Biologiche e Ambientali (DiSTeBA), Università del Salento, 73100 Lecce, Italy
* Correspondence: vcs@ufc.br

Abstract: Aeolian features framed as foredunes worldwide, whose classification faces challenges to separate wave-formed from aeolian ridges, are relevant to the context of anthropic control. An example of this kind of morphology, previously classified as foredunes, is arranged along Brazil's northeastern coast, and the pertinence of its classification as such or even as truly developed dunes was examined. To contribute to the debate on this issue, detailed geomorphological mapping was carried out through UAV and LIDAR surveys, in addition to the multitemporal study of satellite images and aerial photographs. Ground penetration radar sections, trenches, and particle size analysis were also conducted. Although the obliquity of wind direction to the coastline, this study's main bedform of focus shows coast-parallel positioning conditioned by the exogenous vegetation previously inserted about 70 m from the high tide line. This morphology showed practically no migration for over 15 years; however, the wind breaks through the vegetation barrier and develops depositional lobes and V-shaped low crests protruding into the mainland. GPR sections reveal cross-strata sets with a high dip angle in only two aeolian sequences, one preceding exogenous vegetation introduction and the other in a contemporary layer, amidst the dominance of horizontal to sub-horizontal strata. The sediments are characteristically aeolian, with cross-strata and morphology resembling incipient protodunes and a few stretches at the lee slope highlighting characteristics of retention or precipitation dunes. There was little similarity to the foredunes compared to the other occurrences along the equatorial northeast coast; there was also an inconsistency in the correlation between the cross-strata and the morphological stage. In addition, the disconnection between the aeolian dynamics and morphogenetic process also differentiates it from regional foredunes. This morphology, therefore, presents aspects that are not characteristic of the classification of foredunes or the naturally formed dunes in the region and thus demands a classification to emphasize the anthropogenic character.

Keywords: foredunes; human activity; cross-strata; anthropic ridge

Citation: de Carvalho, A.M.; Claudino-Sales, V.; Lima Junior, S.B.; Eduardo, L.M.; da Costa Gastão, F.G.; de Souza Pinheiro, L. Should Anthropic Ridges Framed as Foredunes Be Considered Real Dunes? *Geosciences* **2022**, *12*, 364. https://doi.org/10.3390/geosciences12100364

Academic Editors: Jun Cheng, Felix Jose and Jesus Martinez-Frias

Received: 11 August 2022
Accepted: 26 September 2022
Published: 30 September 2022

1. Introduction

Natural sandy ridges formed parallel to the coastline and along the backshore zone or in its vicinity can vary between those entirely wave-formed, those by aeolian deposition within vegetation defined as foredunes [1,2] a combination of both, or even those formed by human interference.

The occurrence of such morphology formed by the wind action along the coast of Northeast Brazil draws attention for not presenting in satellite and UAV images, as well as in fieldwork, which are the classic characteristics of what is conventionally defined as foredunes. However, these ridges have been mapped as foredunes by public institutions in charge of environmental management and are described in technical reports [3,4]. Therefore,

as these mappings involve matters of environmental management, they consequently comprise legal issues anchored in a classification still in question. It is noteworthy that the supposedly aeolian morphologies arranged close and parallel to the shoreline have historical difficulties in being accurately distinguished from those formed entirely by the wind, waves, or both [5].

Foredunes as generally shore parallel, vegetated ramps, terraces, and convex ridges separated by concave swales [6]. He points out that foredunes are typically the foremost vegetated sand dune formed on beaches' backshore zone by aeolian sand deposition within vegetation.

Other dune types may occupy the foremost position, especially on eroding coasts; consequently, not all of the foremost dunes are foredunes [2,6,7]. In this sense, the term foredunes to the situation in which coastal strand plants can establish themselves in numbers sufficient to fix the ridge as a primary dune structure [8]. However, he questions the vague use of the term to designate any kind of dunes parallel to the coast, which questions its usefulness. Foredunes usually can be formed at the upper limit of wave action on prograding beach platforms, where plant colonization acts in trapping windblown sand [9]. The foredunes are also a consequence of aeolian sediments deposited on backshore by the presence of wrack and wood debris, as pointed out by many authors [1,2,10–15].

The idea that foredunes establishment is linked with the imprisonment of sand with the concomitant growth of vegetation has also been recurrent in literature [8,15–23]. The impact of plant density, shape, distribution, and height on the wind/sand flow are important [2]. Furthermore, the relationship between sand transport and vegetative biophysical feedback responsible for the growth of foredunes has also been well-studied [1,2,24–29].

As for the participation of anthropogenic actions, the foredune development on the Pacific Coast was due to the introduction of marram grass [8]. Thus, the introduction of exogenous vegetation strategically implanted parallel to the coast seeking to stop wind-generated sediment flow can alter wind action and create a morphology that simulates foredunes. Still, its positioning on the beach could lead to even more questions about its classification.

Human interference processes for the formation or expansion of foredunes have been carried out in many coastal regions [30–40] and also with the focus of coastal protection and as result of beach nourishment [41–47]. Therefore, the focus of this work was to gather data to assess whether certain ridges parallel to the coastline, especially those under the known anthropogenic influence, may or may not be properly classified as foredunes or even as true dunes. For this purpose, a set of techniques involving the evaluation of morphological characteristics, position related to the beach face, internal structures architecture, and the history of wind morphodynamics along the coast were applied.

2. Study Area

The study site of this research is located along the 370 km of Ceará coast, Northeastern Brazil (Figure 1). The detailed study area in Cumbuco Beach adjoining Fortaleza City, the capital city of Ceará State, is represented by three different situations of a coastal stretch under intense wind action. This main coastal stretch is controlled by an alignment of exogenous vegetation anchoring the sediments carried by the wind and forming a narrow, elongated, and partially vegetated ridge, which is separated from the high tide line by approximately 70 to 80 m (Figure 1). This alignment extends for about 3 km parallel to the beach, and about 300 m of this is positioned in front of a resort, and about 2.7 km is in front of an unoccupied area. To the east of this area, a stretch without the presence of this vegetation line and without effective occupation of the backshore is highlighted. Five other stretches of the coast of Ceará, in the localities of Porto das Dunas, Beberibe, Taíba, and Flecheiras (Figure 1), were studied as a comparison for the areas detailed in this study.

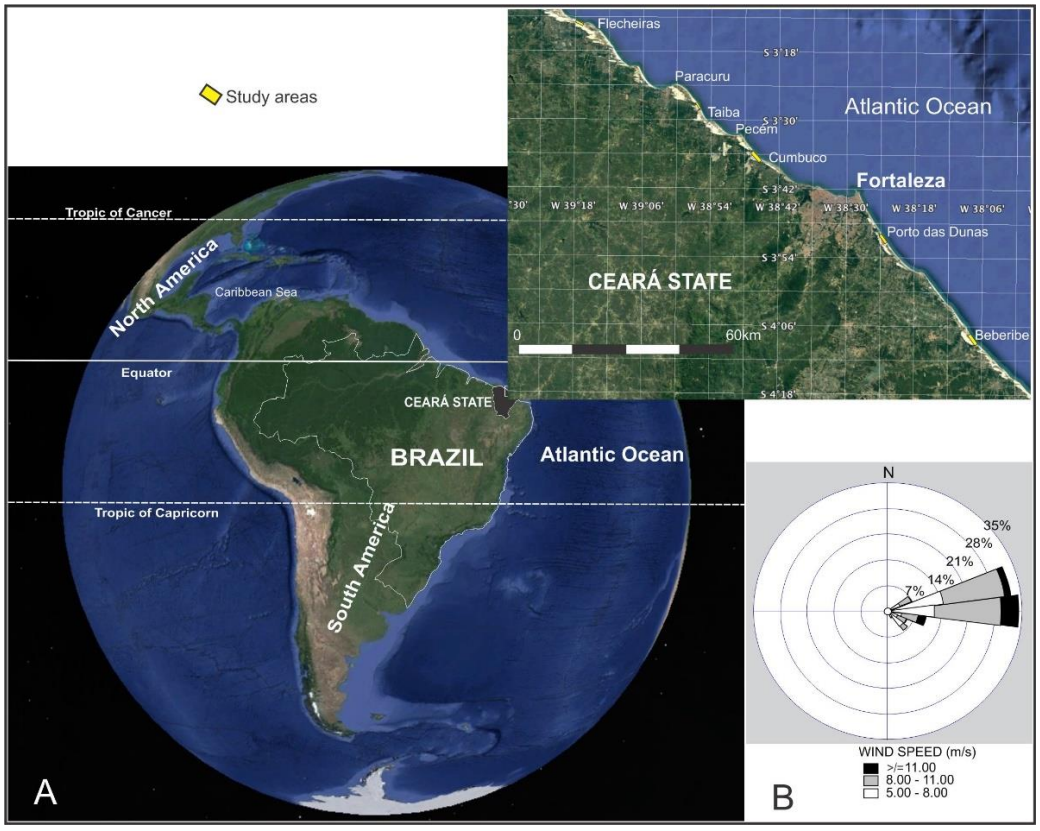

Figure 1. Location map showing the studied stretches of the coast (**A**) and wind regime (**B**) [48].

2.1. Climatologic and Oceanographic Factors

The region is highly influenced by the Southeast Trade Winds, the El Niño Southern Oscillation (ENSO), and the Intertropical Convergence Zone (ITCZ) [49], delimiting an average rainfall of around 1243 mm/y, mainly distributed through the period of February to May.

The rainy season usually starts in December, intensifies over the following months, and reaches a peak between February and June. From there, it describes a decreasing trajectory with minimums between October and November. The winds also have a seasonal distribution, with the low-speed values from January to June, with the lowest values seen in March and April, and the highest ones between July and December, with peaks between August and September. The evaluation of wind direction and speed main averages, considering the data measured in Cumbuco, Pecém, and Paracuru localities, shows the most common wind directions are those from the ESE quadrant, followed by the E quadrant. Other wind directions did not have a significant occurrence and are often associated with periods of greater rainfall, which in theory decreases the effectiveness of transporting sediment. Sand roses along the Ceará coasts indicate the unidirectional easterly winds (Figure 1), with RDP/DP values close to 1 and average drift potential of about 692 v.u. [48,49].

The average annual temperature for the last 26 years, measured at FUNCEME station in Fortaleza, is in the range of 27.3 °C, with a maximum of 32.4 °C and a minimum of 26 °C, producing a maximum range of variation around 6.4 °C.

The tidal regime in the region can be characterized as mesotidal, associated with a semi-diurnal periodicity.

Main wave directions with the respective heights and periods affecting the study area are N25°, with heights of 1.0 to 1.5 m and periods of 5.0 to 6.5 s; N60°, with heights of 1.0 to 1.5 m and periods of 5.0 to 6.5 s. Swell waves (period 10 to 20 s) comprised 28%, while sea waves (period 1 to 9 s) reached 72% of the occurrence over one year, of which 58% of the periods were concentrated in the range of 4 to 7 s [50].

2.2. Geology and Geomorphology

The area consists of a stratigraphic sequence represented by Precambrian unities in its base that outcrop into the Cumbuco and Pecém headlands (Figure 1) and are overlapped by Cenozoic sequences constituted by deposits of the Barreiras Formation in addition to colluvial and eluvial cover [51] Finally, at the top of this sequence are the quaternary units represented by fluvial, aeolian, and beach deposits.

The geomorphology of the region combines beaches ranging from Reflective plus Low Tidal bars and rips (R + LTR) to Reflective plus Low Tide Terrace (R + LTT) [52]. The presence of a reflective high tide beach and a more dissipative beach at low and intermediate tides are very common on all the R + LTR beaches. Beach face scarping commonly occurs at high tide but with minimal changes in the beach face. Aeolian terraces are represented by active and stabilized deflation plains and fixed and mobile dunes. The most anthropized area in question is characterized by fine to medium sand, predominantly aeolian. The aeolian surface varies from 500 to 5000 m in extension landward, with many dunes positioned obliquely to the coastline. In some segments, for which this study case is a perfect example, the coastline position favors sediment mobilization by the wind flowing towards the continent, originating dune fields with past migration over 10,000 m inland [51], a process that is still recorded by the presence of stabilized vegetated dunes.

2.3. Coastal Dynamics

To better understand coastal dynamics on the coast of Ceará, it is appropriate to divide it into segments according to the predominance of specific processes (Figure 2). Wave diffraction predominates over wave refraction along the segment with the most significant curvature of the bays immediately downstream of the promontory, called "first segment" [51], and is based on beach equilibrium [53–55] (Figure 2). In this segment, there is intense feedback on the beach from the sediments transported by the wind from the upstream-facing of the promontory into this area. In the second segment, which presents a straighter coastline than the segment above, the wave refraction process predominates, with a tendency to hit perpendicular to the coastline, minimizing drift transport in taking more sediment available for wind transport towards the interior of the continent [51,56] (Figure 2). There is a relationship between winds and shoreline orientation for the coast in southern Brazil, wherein the foredune volume is at a minimum in the greatest bay curvature of the beach and at a maximum in the smoothing curvature stretch of the coast [57].

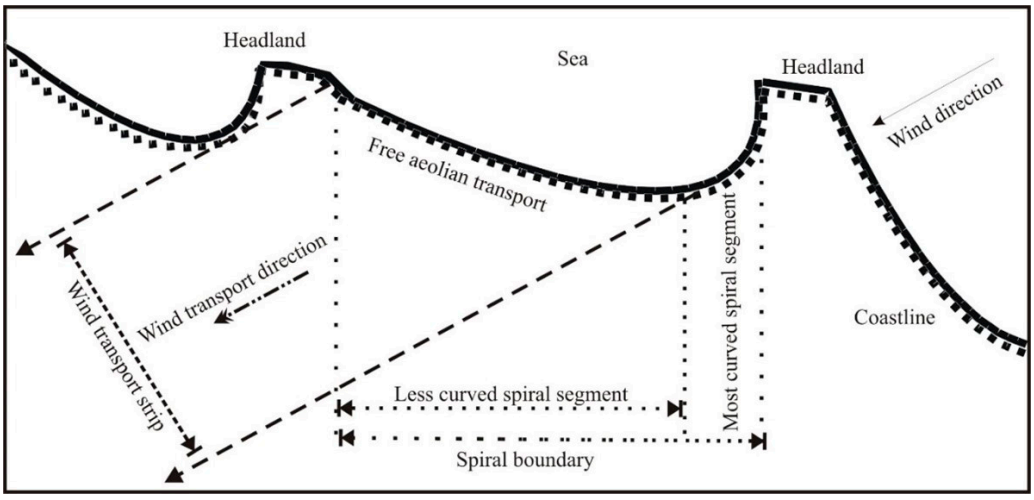

Figure 2. The conceptual model for coastal morphology shows the variation in the coastal segment and its relationship with aeolian transport and foredunes formation (modified from [51]).

3. Methods

3.1. Ground Control Points (GCPs) Determination

Eleven GCPs were set, and their precise geographic location was obtained using RTK (Real-Time Kinematic system) geodetic GPS. The GCPs and the reference points for further geographic rectification were marked with a 50 cm × 50 cm black mat with a white "X" painted at the center (Figure 3).

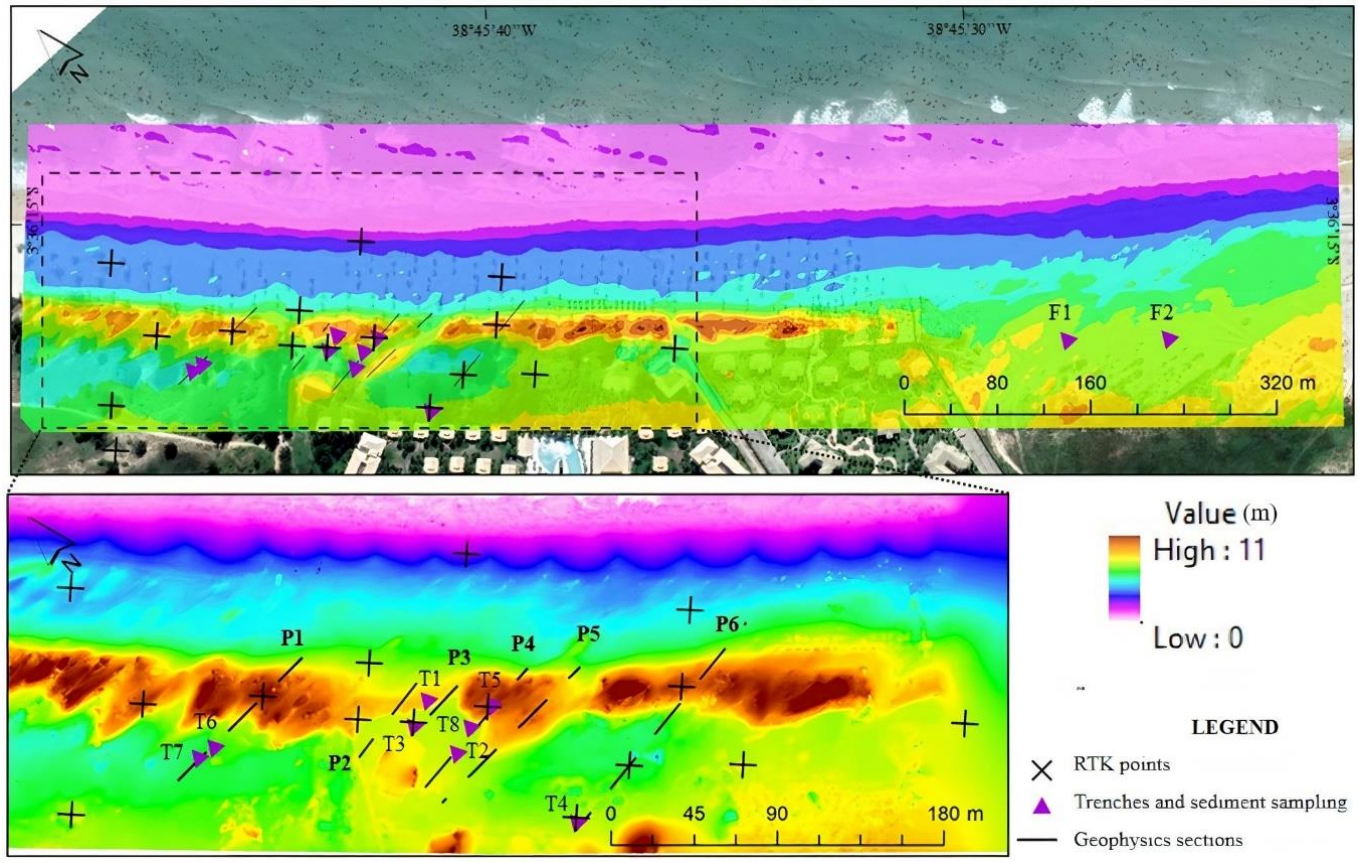

Figure 3. 3D map locating RTK points, treches (T1 to T7) and GPR sections (P1, P2, P3, P4, P5 and P6).

After the field data acquisition stage, the control points were adjusted to ellipsoidal height and horizontally corrected by triangulation based on the information from two altimetric stations of the Brazilian Network of Continuous Monitoring (RBMC). Using MAPGEO 2015, free software from the Brazilian Institute of Geography and Statistics (IBGE), altimetry and geoidal undulation were verified, in addition to the conversion of geometric RTK data to orthometric values related to mean sea level.

3.2. Multitemporal Image Processing

In order to carry out the multitemporal study, a survey of the Landsat/Copernicus satellite images available from 2004 to 2018 was carried out. These images were processed and georeferenced in a GIS environment on the SIRGAS2000/UTM ZONE 24S datum. Data from the RTK Geodetic GPS measure in the study area were used to refine the georeferencing of these images.

In addition, imaging was also performed associating a UAV and RTK survey, leading to the development of a digital elevation model (DEM), as described below. The resulting DEM served as an altimetric basis to compare the evolution of wind morphologies and to define elements of association between such morphologies and characteristics of textures, as well as the roughness of the satellite images.

3.3. UAV Data Acquisition and Analysis

The flight mission was carried out on 8 January 2019 under good meteorological conditions. A flight plan was produced previously in the lab. The input of information related to flight altitude (135 m), lateral and longitudinal overlap (80%), velocity (11 m/s), and the insertion of waypoints guided the route of photogrammetric coverage through an area of 0.18 km^2 with five coast-parallel lines and 71 acquired photographs. For this purpose, was used a Phantom 4 DJI (Da-Jiang Innovations Technology Co) with a DJI FC330 camera of 4000 × 3000 pixels resolution, 6.17 mm × 3.47 mm CMOS (complementary metal-oxide semiconductor) sensor, and 3.61 mm focal length.

Adjustments of the images' coordinate system generated by aerial photographs with the terrain coordinate system were conducted using 11 control points (PCs) in the field (Figure 3). Three were used as verification at the end of the processing and generation of cartographic products. Similar to the satellite images, the horizontal information used for UAV data was SIRGAS 2000/UTM Zone 24S.

Residual errors for the X (Easting), Y (Northing) and Z (Altitude) axes of all control points were calculated from about a total error of 5.42 cm, translating into a pixel dimension accuracy of 0.83 cm.

The processing of area photographs acquired by UAV was performed using the OpenDroneMap software, allowing the creation of DEM, DTM and Orthomosaic, the main products of this type of work.

Next, the phases of camera alignment and point cloud formation were carried out, creating 121,803 tie points. The alignment of photos and the generation of tie points was of fundamental importance for the generation of densified point clouds and the subsequent creation of 3D models, in addition to being a point of connection between the orthophoto in the process of creating the mosaic.

A general election was made to exclude parts of the terrain that did not contribute to the processing and generation of orthophoto and models, such as seawater strips and the entire area's North, South, East and West side edges. This process was followed by the insertion of Ground Control Points (GCPs) acquired in the field, a step in which the positional accuracy of the point cloud is adjusted and improved based on a series of geometric corrections. A high-resolution Dense Point Cloud was generated next, resulting in 15,318,446 points and contributing as a base for DEM and Orthomosaic generation. From the DEM, the data was filtered, classifying different elements within the terrain, leaving only the data necessary to generate the DTM. In this last stage, Orthomosaic was created, and all the final products were used to map the geoenvironmental units of interest.

3.4. Internal Structure Using Trench and GPR

Subsurface data were acquired through electromagnetic and manual methods. To understand superficial internal sedimentary structures, eight trenches up to 30–50 cm deep were excavated in strategical stretches of the study area, where the layering pattern could reveal interesting aspects to the classification of the morphologies. Some of them, including trenches T2, T5, T6, T7, and T8, were excavated throughout geophysical profiles (Figure 3), aiming to match both results. Trench T1 is on a slightly elevated depositional surface, while T3 is located at what once had been a lee projection of the previous feature. Trench T4, located nearby profile P6, marks a reference to the stabilized deflation surface leeward of the likely retention dune.

Furthermore, to enhance internal structure interpretation and corroborate conclusions based on the UAV-generated models, six geophysical sections were performed using Ground Penetration Radar (GPR). This method consists of a high-resolution sampling technic based on the reflection of electromagnetic waves [58,59]. The equipment used was a GSSI (Geophysical Survey Systems, Inc., Nashua, NH, USA) model SIR-3000 with 200 and 400 MHz antennas, which can measure depths up to 8 m on dunes. All sections were performed with a constant spacing sampling of 40 traces per meter. When processing these data, a velocity of 0.113 m/Ns determined from diffraction hyperboloid analyses

with ReflexW 5.0, Licence Number 639 (©Sandmeier Scientific Software) was obtained for the shallow sediment cover that allowed for the parameterization of GPR depths with a mean dielectric constant of 6.94.

Due to the marked relief, topographical corrections were conducted on the GPR sections using a RTK Geodetic GPS.

The data processing mechanism followed the routine which includes: (i) data editing, (ii) signal treatment, and (iii) presentation of the processed image [60].

GPR section number one (P1) took place on the west side of the detailing area, covering a 90 m long transect. Sections P2 and P3 have around 50 m, while P4 and P5 were, respectively, around 90 m and 100 m long (Figure 3). Finally, section P6, located on the east side of the detailing area, had the longest profile of about 140 m (Figure 3).

3.5. Particle Size Analysis

The subsurface and surface sediments were sampled in trenches along with the six profiles and at the east of the exogenous vegetation crest along the study area, in a total of nine sediment samples (Figure 3).

Sediment samples were dried to determine grain size by gravimetry analysis [61]. The samples with 100 g were wet-sieved to separate the mud fraction from sand and gravel. The mud's fraction was less than 10%. The grain size analysis was carried out at 1 phi intervals with a mechanical agitator for 10 min at a frequency of 10 Hz. Therefore, a sequence of sieves of different meshes was used [62].

To obtain the granulometry data and statistical parameters, the SISGRAN software was used [63]. The statistical parameters used were those of Folk and Ward [64] and provided a good application of the sedimentology of beaches and dunes.

4. Results

4.1. Geomorphology and Morphodynamics

Across from the resort area and extending westward, there were exogenous vegetation (*Casuarina equisetifolia*) and coconut tree alignments parallel to this coastline, implanted in the 1960s, and it is also supported by the gradual expansion of native vegetation colonization verified in the multitemporal study of satellite images and photographs acquired by UAV.

The stretch between the foreshore and upper part of the backshore, mainly along the resort strip (Figures 4 and 5A), is under an active deflation process. It is likely to be largely due to the heavy traffic of vehicles [65,66], as well as constant touristic activities. In addition, over the years, no work has been identified aiming at the artificial construction of dunes along this stretch, such as beach scraping [67,68]. On the other hand, along the stretch of exogenous vegetation alignment, relatively far from the swash zone, a sandy ridge was formed parallel to the beach line fed by sediment inflow brought by the wind to the backshore's highest portion (Figure 4). The stabilization process of this aeolian crest occurs with greater intensity throughout the area in front of the resorts, where implantation and gardening maintenance are seen to fix sediments dispersed by the wind. This crest presents itself in isolation, consequently without the development of swales. The evolution of the vegetation cover from 2004 to 2018 on this crest parallel to the beach (Table 1) shows an increase in the vegetation cover between 2004 to 2012 and a decrease between 2012 to 2018, with an increase in the crest area associated with a possible decrease in vegetation cover.

Table 1. Evolution of vegetation cover from 2004 to 2018.

Year	Crest Area (CA)	Vegetal Cover (VC)	%VC
2004	21,862.05 m^2	7632.34 m^2	34.91%
2012	13,496.89 m^2	8568.88 m^2	63.49%
2018	14,977.08 m^2	8204.49 m^2	55.15%

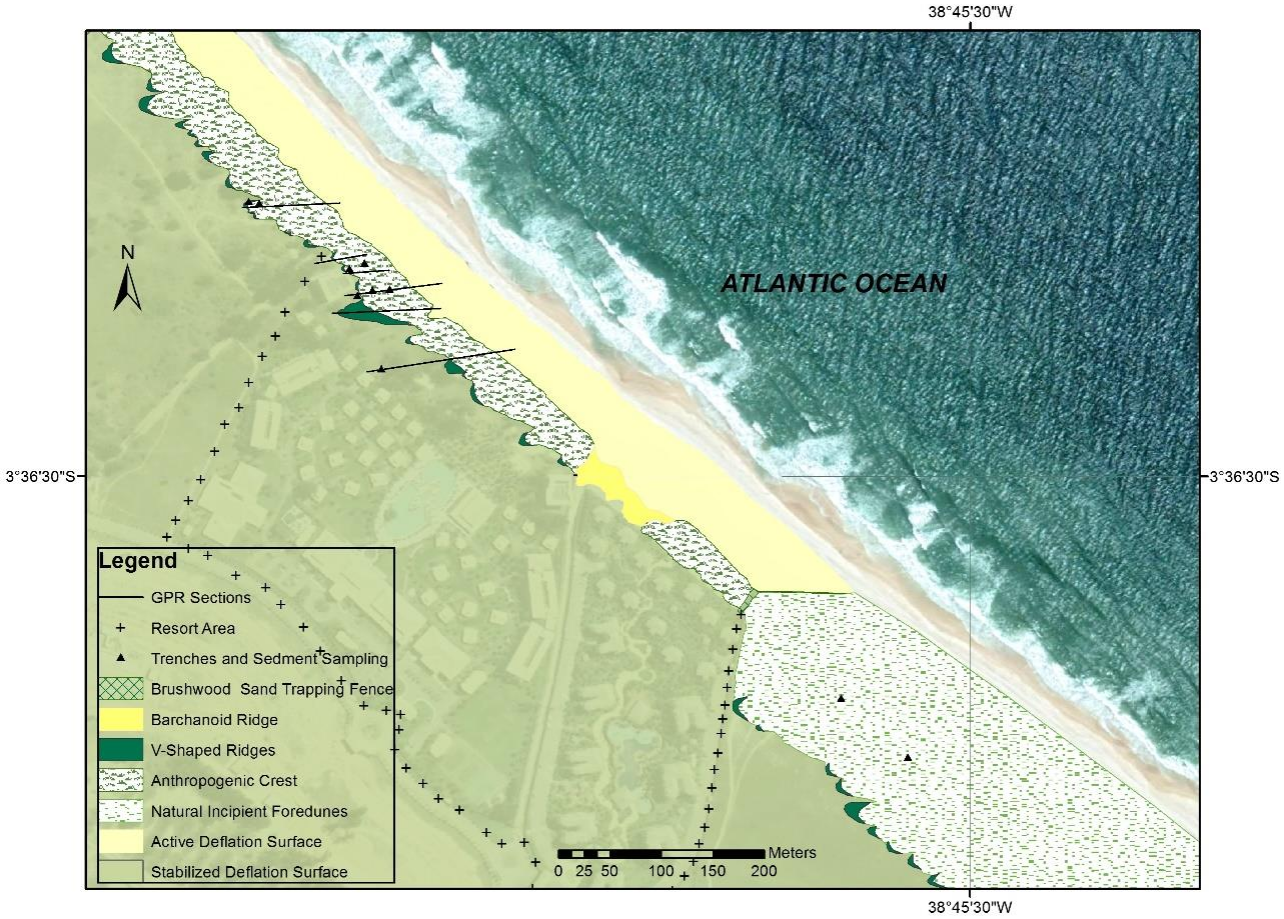

Figure 4. Morphological map showing the anthropogenic crest parallel to the beach, on which the vegetated stretches separated by preferential corridors of wind/incipient blowouts stand out. The active deflation surface to windward, and the stabilized deflation surface and the low V-shaped ridges the leeward. To the east, the incipient natural foredunes stand out.

In many stretches along this crest parallel to the beach, the wind can excavate areas between vegetation cover and develop preferential wind corridors. In these stretches, wind causes the formation of deflation channels or incipient blowout and, to the leeward side, depositional lobes and low V-shaped ridges (V-s R) (Figures 4 and 5A,B). Eventually, these deflation channels highlight more densely vegetated cover mounds (Figure 4), in some cases producing morphologies similar to nebkhas.

The data show that interaction between vegetation and wind transport has a seasonal character. Therefore, there was less wind transport and expansion of the vegetation cover area during the rainy season, with the opposite occurring during the dry season. In addition, the evolution of aeolian morphologies from 2004 to early 2019 shows the crest parallel to the beach, and the low V-shaped ridges have practically not migrated for 15 (fifteen) years. These morphologies remain around the boundary of the exogenous rectilinear vegetation alignment implanted parallel to the coastline.

Along the stretch where the exogenous vegetation alignment was implanted, the formation and evolution process of low V-shaped ridges and preferential wind corridors has been unable to develop true downstream dunes, but only sand dissipation ducts on the stabilized deflation surface. Subsequently, these sediments are covered with vegetation during the rainy season.

Figure 5. The photographs shown in Figure 5 (**A**–**E**) show low terraces formed by the dissipation of sand along preferential wind corridors, producing low V-shaped ridges (**A**,**B**) and depositional lobes (**C**), sandy terraces over the stabilized deflation plain (**D**), and retention or precipitation sandy deposits, as well as lobe deposits, (**E**) Cumbuco Beach.

The photographs in Figure 5A–C show low terraces formed by sand dissipation along the wind corridors, producing low V-shaped ridges and depositional lobes. Part of the sediments, transported beyond the leeward limit of the ridge parallel to the beach, are dissipated, developing sandy terraces over the stabilized deflation plain (Figure 5D). In addition, small retention or precipitation sandy deposits (Figure 5E) are occasionally developed [69]. However, this process occurs more often along the stretch west of the resort area (Figure 1), where incipient slipfaces precipitate sediment around and over trees and shrubs (Figure 5E). Nevertheless, this type of deposition does not occur in the area east of the resort stretch (Figure 1).

The morphological evolution is completely different along the area east of the resort, which is not under the influence of the exogenous vegetation line (Figures 1 and 4). In this section, a small ridge truncated by the waves from the spring high tide zone is observed (Figure 6A). From this zone, continent inward, an aeolian surface develops partially covered by native grassy vegetation, with some stretches lowered by wind deflation (Figure 6B), whose characteristics match incipient foredunes model [2], which is also known as 'embryo dunes' [64].

Figure 6. (**A**) Ridges parallel to the beach line cut by the waves on the windward face of the incipient foredunes; (**B**) incipient foredune experiencing a deflation process; (**C**) stretch of vegetation cover growth and formation of incipient nebkhas; (**D**) stretch of farther formation of crests oblique to the beach line. Cumbuco Beach.

This morphology extends inland for about 70 m with minor changes in morphological characteristics and vegetation cover (Figure 6C). In and around this 70 m, small vegetated mounds like nebkha features (Figure 6D) [70–73], vary from the juvenile to the mature stage [7]. Adjacent to the transition stretch of this incipient foredune, with the stabilized

deflation surface, dense and largely shrubby vegetation obliquely oriented to the beach line is present and develops V-shaped crests (Figure 6D) at around 80 to 100 m. These incipient internal limits of the dunes correspond approximately to the distance in which the exogenous vegetation (*Casuarina equisetifolia*) alignment, parallel to the beach in front of the resort, was positioned (Figures 4 and 6C). In the multitemporal study of satellite images, these incipient foredunes advance beyond the limits of the aforementioned line of exogenous vegetation.

The exogenous vegetation line does not directly influence this east area. Still, it is also impacted by the traffic of traction vehicles, which favors sand mobilization and interfere with vegetation cover stabilization.

Elsewhere along the coast, such as in a stretch to the west of Taíba locality (Figure 1), in an attempt to impede sandy aeolian transport to an area subdivided for urban occupation, the placement of parallel tree trunks and brushwood branches in a pile above the berm line produced an accumulation of sand ridge parallel to the beach. Additionally, this sand accumulation developed V-shaped ridges oblique to the beach (Figure 7), similar to what is seen in the focus area of this study, as well as in natural stretches of the Brazilian Northeast coast, but still without vegetation cover.

Figure 7. Distribution of branches and tree trunks parallel to the beach in the high tide strip with consequent development of foredune-like morphology with V-shaped crests oblique to the coastline. (**A**) Photographed in the west direction and (**B**) in the east direction. Taíba Beach.

Satellite and field studies show foredunes commonly experience deflation processes, developing small blowouts (Figure 8A) or larger blowouts (Figure 8B), such as in Porto das Dunas (Figure 1). This is a common coastal process on both eroding and accreting coastlines [2,74]. It is likely that, eventually, this process can evolve to form parabolic dunes and/or places of sediment accumulation serving as embryos for barchan and barchanoid dunes generation. This occurs when the capacity of sand retention by the vegetation is exceeded by the volume of sediments carried by the wind. The increase in the volume of sediments downstream may be sufficient to initiate isolated dunes and transgressive dune fields.

Figure 8. (**A**) Satellite image showing three stages of the blowout evolution; a current blowout zone; a stretch with a blowout in a stabilization stage; blowouts already stabilized, showing remnants of parabolic hairpin dunes downstream. (**B**) Development of blowout on incipient foredune. Porto das Dunas beach.

The development of established foredunes with concave swales is also not common in this region. However, in a coastal stretch along the Beberibe (Figures 1 and 9), a long ridge with vegetation cover was observed positioned immediately at the beginning of the less curved bay segment (Figure 2). This crest represents an example of a more established foredune stage observed in this region, which is supported by vegetation cover that is not larger than the shrubs (Figure 9).

Figure 9. Foredune in Beberibe beach (see Figure 1) of about 4 m high and 50 m wide. (**A**) Photograph in the west–east direction, showing two points of sediment advancement over the vegetation. In the background, the promontory and the urban occupation in the surroundings are observed. (**B**–**D**) Photographs from east to west forward show the variation in vegetation cover (**B**) and the incidence of sedimentary flow covering part of the vegetation surface (**C**), as well as the formation of a small incipient blowout and development of depositional lobe downstream (**D**).

On the other hand, along a stretch of Flecheiras (Figure 1), the incipient foredunes stand out as lowered surfaces and are partially covered by undergrowth. This surface is marked by sand shadows (Figure 10A) and larger elongated ridges parallel to the wind and oblique to the beach, with partial vegetation cover (Figure 10B). These ridges and sand shadows are separated between themselves by recessed surfaces and/or deflation surfaces.

Figure 10. (**A**) Sand shadows on lower insipient foredune; (**B**) incipient foredune highlighted by elongated ridges parallel to the wind and oblique to the beach in Flecheiras.

4.2. Sedimentology

Sediments on the surface of the incipient foredunes to the east of the resorts are well-sorted medium sand (samples F1 and F2, Table 2).

Table 2. Statistical parameters and classifications were obtained for samples F1, F2, T1, T2, T3, T4, T5, T6, and T7.

Sample	M_{d_Φ}	S_{ki_Φ}	K_{g_Φ}	S_{i_Φ}	Folk & Ward Classification
F1	1.667	−0.040	1.023	0.489	Well-sorted medium sand
F2	1.747	−0.025	0.846	0.492	Well-sorted medium sand
T1	1.701	0.008	0.947	0.455	Well-sorted medium sand
T2	1.788	−0.032	0.890	0.462	Well-sorted medium sand
T3	1.830	−0.083	0.856	0.476	Well-sorted medium sand
T4	1.748	−0.028	0.907	0.702	Moderately sorted medium sand
T5	1.851	−0.051	0.882	0.439	Well-sorted medium sand
T6	1.690	0.016	0.971	0.427	Well-sorted medium sand
T7	2.133	−0.217	0.996	0.373	Well-sorted fine sand

In the trenches along the crest parallel to the beach, in front of the resort area (Figures 3 and 11), there is a sedimentary cover composed of fine to medium sands, and the subsurface strata (excavated to about 30 cm in depth) are generally composed of well-selected medium sand (Table 2). Only the samples from the T4 trench are represented by moderately sorted medium sand, and from the T7 trench, which is characterized by well-sorted fine sand (Table 2). This last case represents a distant portion from sand dispersion inland over the stabilized deflation surface (Figures 3 and 4).

Figure 11. Trenches show planar strata T1, T5, T6, and T7, cut in almost stabilized deflection surface. The presence of roots and fragments of vegetation, and a soil level in the sections dug on the stabilized deflation surface (T2, T3 and T4) and also in T6. T8, trench cut into the face of an active depositional lobe. Cumbuco Beach.

Along the stretches in which trenches were excavated on the stabilized deflation surface, as in the trenches T2, T3, T4, and T6, soil levels of about 5 to 10 cm thick are usually intercalated by thin layers of sand; this aspect is well represented in T6 (Figure 9). In the T7 trench, soil development is very incipient.

4.3. Sedimentary Structures

The sedimentary deposits observed in trenches (Figure 11) have plane-parallel strata ranging from horizontal to sub-horizontal. Usually, the roots, many vegetation fragments, and/or intercalations of sand and horizons with soil occur. In trenches T1 and T5 (Figures 3 and 11) cut over the aeolian crest, there are thin, sub-horizontal sets with

a small downwind dip angle and the presence of current aeolian ripples on superficial sub-horizontal sets in T5. In some stretches of the trenches dug on the leeward face, such as the T8 trench, an incipient slipface developed with high dip strata (Figure 11).

In the GPR sections (Figures 3 and 12), Profile P1 presents a section with low dip angle sets, generally following the previous topography or the successive accumulation of sediments on a stretch of higher relief. Most sets dip at low angles toward the sea on the windward side and flatten out on top of the ridge. On the leeward face, sets dip smoothly with a low landward-dipping until they become horizontal along the stabilized deflation surface. At about 2 m deep in the P1 profile, below the hydrostatic level (Figure 12), a long sequence of sets (of about 60 m) of high dip angle cross-strata is highlighted. These cross-strata sets were truncated at the top, possibly spared from total erosion by aeolian deflation due to the presence of hydrostatic level.

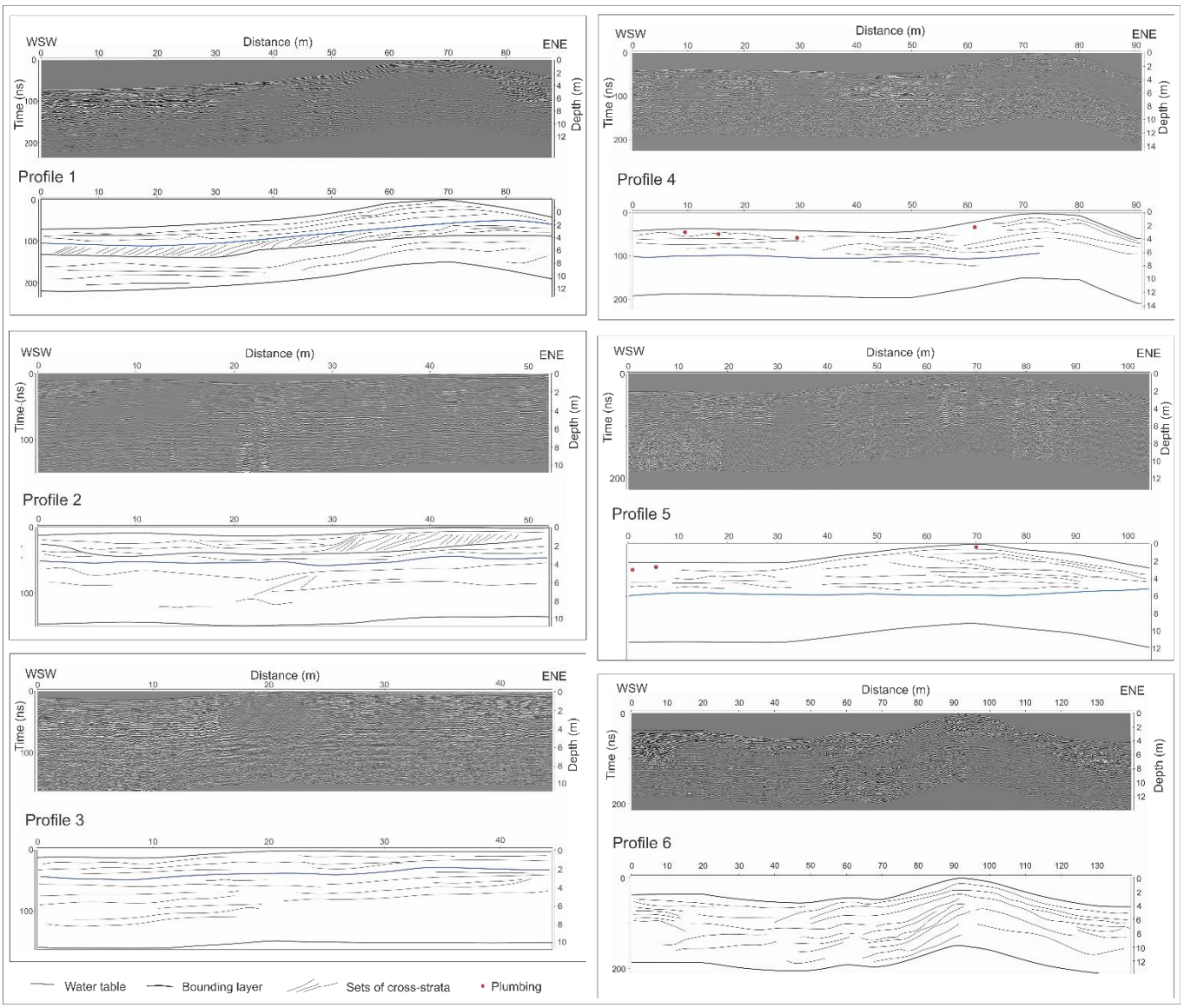

Figure 12. GPR sections processed and interpreted from profiles P1, P2, P3, P4, P5 and P6 (See the location of profiles in Figure 3). Wind direction from ENE to WSW, from the right to the left of the images. Cumbuco Beach.

Profile P2 (Figure 12) started from the beach side of the crest to the landward side. The strata are smooth with horizontal to sub-horizontal dips, with apparent deflation and

filling sets between the points of 0 and 50 m. However, it displays a stretch between points 30 and 50 m, with high dip angle sets covered by a thin horizontal sandy layer. This last layer is the result of a fairly recent migration of a small slip face formed after the removal of vegetation from this stretch. These sets rest on sub-horizontal ones, and then a continuous sub-horizontal water-table reflector appears, as in profile P1. Small sets with high dip angles seem to be repeated just below the water table, between 20 and 30 m. This stretch presents a photographic history of a seasonal deflation surface.

Profile P3 (Figure 12) extended from the top of a lowered section (under deflation) on the ridge parallel to the beach to the sidewalk of the resort building (Figure 3). This section is even and fairly monotonous with horizontal to sub-horizontal sets, such as the WSW portion of the P2 profile and the T3 trench (Figure 11).

Profile P4 (Figure 12) extended from the windward face of the ridge parallel to the beach until the vertex of a resort building (Figure 3). Like the other profiles, this one is characterized by the monotony of stratifications, which sets a dip following the pre-existing topography. It presents plane-parallel stratification, with a high dip in the windward and leeward faces of the ridge parallel to the beach. The sets are horizontal at the highest portion of the crest, which is similar to what occurs in profile P1, but with discontinuous, concave, and convex-up reflectors on top of the crest and along 0 to 30 m and from 35 to 60 m. At about 60 m, the sets with a contact similar to the onlap are highlighted. In Profile P4, the lowered leeward surface rises smoothly, dipping seaward and then landward as sand dissipation flows over the stabilized deflation surface.

Profile P5 (Figure 12) extended from the windward face of the ridge parallel to the beach, crossed its top and continued over the entire low V-shaped ridge (Figures 3 and 5A). This low V-shaped ridge (see Figure 5A) is the longest and most persistent of the studied area. Until reaching the limit of the water-table level, profile P5 is very similar to profile P1. Strata are mostly plane-parallel and basically follow past topography. The sets with smooth dip angles dip windward and seaward of the ridge parallel to the beach. This profile also shows a pattern of horizontalizing layers after facing leeward over the stabilized deflation surface. Then, along a V-shaped ridge, a gentle slope dipping seaward and leeward was acquired. This resembles the deposits in the reattached flow zone [75]. In the stretch between 60 and 70 m, a set contact similar to the onlap was observed, which seems to be a leeward face that advances over the previous stoss slope of an aeolian sedimentary sequence, or is just a trough cut and fill on a previous crest.

Profile P6 (Figures 3 and 12) was the longest and was quite monotonous, presenting predominantly plane-parallel strata, horizontal to sub-horizontal, with dipping strata following the previous topography. It also showed concave and convex-up reflectors landward and seaward of the ridge parallel to the beach. In the section between 70 and 90 m, strata similar to an incipient slipface with characteristic similar to retention ridge is observed. This profile also crossed a small depositional lobe (see Figure 5B) in the stretch between 50 and 70 m. This lobe was partially covered by a horizontal leeward layer (Figure 12).

5. Discussion

Wind dynamics on the coast of Northeastern Brazil show that oblique onshore winds intercept the coast. Therefore, the pattern of foredunes produced by onshore winds perpendicular to the beach line is not characteristic of the coast in Northeast Brazil, which is more fitting to an onshore oblique, attached-deflected wind [76,77]. These winds perpendicular to the beach accelerate more often [78]. Still, their performance results in low aeolian mass fluxes that reach a maximum at the dune foot, while the oblique winds are more effective in transporting sediment from a foredune's foot to its slope.

This aspect is associated with the fetch expansion due to the oblique position of the wind to the coastline [79] and is expected to be responsible for the giant wind transport common to the northeastern Brazilian coast. Additionally, the foredunes along this region are generally developed by joining several long successive ridges oblique to the beach line and parallel to each other (Figures 8B and 10B). The truncation of these ridges by wave

action develops a seaward slope in incipient foredunes, producing long ridges parallel to the beach (Figure 6A). As the foredunes advance inland and transit to other types of dunes, the wind behavior along the northeast coast requires a more detailed study.

There are also no significant changes in the migration direction of the dunes formatted in the post-foredune stage. The exception occurs along the stretches of crests interaction in transgressive dunes fields, especially with crescentic overlapping dunes [80]. The area in front of the resorts (Figure 4), from the beach-landward, presents a stretch of backshore that behaves as an active deflation surface resulting from intense human activity. On the stretch to the west of the resort, this deflation area is less active, which may be associated with less human activity. Wind action also produces more precipitating or retention lee slipface associated with fewer human activities, such as maintenance of vegetation cover, which is more effective by dune gardening [81] in front of the resort area.

Along the area to the east of the resort, neither localized active deflation surface nor the formation of a long ridge parallel to the beach far landward of the backshore, as well as no precipitating or retention slipface are found. This indicates differences in aeolian morphology compared to the other stretches controlled by vegetation lines, although also experiencing human activities. In this context, in the case of Taíba Beach (Figures 1 and 2), the introduction of tree branches and trunks along the high tide level stretch produced a V-shaped crest morphology similar to that developed in front of the Cumbuco Resort, but without vegetation and attached to the high tide line.

This morphology resembles the furthest portion from the tide line in the eastern section of the resort. In the latter case, the V-shaped ridges develop with the presence of native vegetation. Therefore, the development of V-shaped crests, with or without vegetation cover, oblique to the beach line and parallel to each other seems to be the pattern of foredune in the region. On the other hand, the development of ridges or foredunes parallel to the beach line observed along the coast is only a result of the seasonal action of waves on the frontal dunes. In contrast, similar types of ridges far from the beach line were observed only in the anthropogenic case of Cumbuco.

Sediments distributed throughout the studied area are predominantly composed of well-sorted medium sands, fitting the pattern of aeolian sands. These sediments transported from the beach by the wind are retained in part as reaching the alignment of exogenous vegetation implanted parallel to the coastline, which are the major conditioning of this ridge parallel to the beach. This type of ridge positioned in the higher portion of the backshore, relatively far from the swash zone, are non-existent along the Brazilian Northeast region. In a natural process, crest height increases and length decreases as plant height increases [1,82]. Additionally, the excess sediment should lead to widespread burial of vegetation as sand is delivered faster than vegetation growth can accommodate, and then sediment bypasses the foredune [83]. In contrast, this local crest parallel to the beach has already been initiated on a line of tree-sized vegetation in a stretch far backshore.

Sand supply primarily affects dune crest height and dominates at the interannual timescale [84]. Beachgrass growth rates are likely too slow to respond to significant variations in sand supply rates at seasonal scales. This matches with the wind transport pattern in the dry season along the stretch in front of the crest parallel to the beach. However, the gardening and the size of exogenous vegetation (*Casuarina equisetifolia*) in front of resorts prevent most of the sand bypass. Therefore, it is more effective in the area west of the resorts, where vegetation is only dependent on climatic conditions. Moreover, human activity on sandy shores, which often restricts sediment budgets, can eliminate landward dune sub-environments and their associated habitats and can limit the space over which natural processes can subsequently rework beaches, dunes, and uplands [85,86].

Satellite images and field studies suggest that a sand bypass occurs through the development of blowout-type processes, especially when sediment inflow by the wind exceeds the vegetation cover's retention capacity. The lower plants reduce the airflow and transport more slowly, so there is a gradual downwind reduction in transport, which

produce asymmetric dunes with a short slope on the downwind side [2]. However, this does not seem to be the case for most of the crest parallel to the beach.

The sand deposition process on the foredune slope occurs when vegetation cover exceeds about 50% of the maximum density measured on the dune crest [78]. In the area of the exogenous vegetated ridge parallel to the beach, it was observed that there seemed to be an increase in the area of this ridge associated with a decrease in the vegetation cover (Table 1). However, this aspect may be associated with the greater wind flow spreading sand around this ridge. Apparently, the smaller crest area associated with greater vegetation cover may correspond to an increase in the height of the crest [8,78].

The expansion of deflation stretches over this ridge parallel to the beach during the dry season basically occurs in places with a lower density of vegetation cover, while the total or partial colonization of stretches during the rainy season has caused a consequent decrease in the wind deflation process [2]. In addition to the seasonal variation in plant density and distribution, the seasonal growth rates strongly influence patterns of sand transport and deposition on incipient and established foredunes [2]. Especially in drought, the wind can excavate stretches between vegetation and develop wind corridors.

The wind velocities experience local acceleration around and flow separation behind the plants [82,87–90]. Locally, between vegetated and bare stretches, the wind develops erosional surfaces (blowout type) associated with leeward depositional features, such as lobes and low V-shaped ridges (Figure 4). This aspect also differs from the area to the East of the resort and along other stretches of the coasts, such as Flecheiras (Figure 10).

Blowout formation or expansion occurs because the vegetation cover is weakened, reduced or eliminated during the arid period [71,73,91,92]. Along the studied region, this process is also favored by the increasing effectiveness of the wind during the drought [51].

A multi-temporal study of satellite, LIDAR and UAV images from 2004 to 2019 showed that the surface of this exogenous vegetation ridge parallel to the beach has characteristics similar to morphological stages 3 to 4 (Table 1 and Figure 5A) but with internal structures (Figure 12) mainly with the stage 1 to 3. However, profile 4 (Figure 12) presents structures suitable for stage 4 [1]. This adds a certain inconsistency between foredunes' morphological and cross-strata stages when analyzing this morphology as a whole. In addition, this crest position is in an unusual backshore space for foredunes in the region, increasing classificatory inadequacy in the context of foredunes.

In addition, the cross-strata in most GPR profiles raise doubts about this morphology as to the definition of well-formed dunes or protodunes [8,93–109]. The cross-strata (Figure 12) are predominantly characteristic of protodunes [97]. Therefore, some stretches to the leeward face show characteristics of retention or precipitation dunes (Figure 5D), which, in some parts, highlight the attributes of transgressive dunes running onto large and medium-sized vegetation. However, it would not be appropriate to define this single rectilinear crest as a protodune without considering some profiles with precipitation/retention crest characteristics. Therefore, it is another aspect complicating its classification in the context of natural dunes.

The large section of cross-strata sets of high dip angle in profile P1 (Figure 12) is probably from a migrating dune slipface. This type of high cross-strata dip is not common to sand accumulated around vegetation [17,110]. Although high cross-strata dip could be developed in a more advanced stage of foredunes [1], this is not suitable for the morphology and history of this crest produced by the implantation of the exogenous vegetation alignment. However, it is likely suitable that its cross-strata were formed before the exogenous vegetation cover line was implanted.

These cross-strata could be developed on a stretch where most of the backshore portion of the natural foredunes used to extend inland, as in the case to the east of the resort. This may indicate the pattern of aeolian transport around the ridge parallel to the beach is distinct from natural processes. Additionally, the development of characteristic slipface cross-strata, as in recent sets identified in profile P2, shows the absence of vegetation can

evolve to the formation of slipface. This aspect indicates that interruption of the anthropic influence in stopping wind transport can easily trigger the formation of migrating dunes.

These disconnected characteristics certainly reflect the absence of a programmed anthropogenic method for foredune formation [111]. It was the product of human interference aiming simply for damping wind transport without the objective of forming a foredune with the purpose of coast protection.

Furthermore, the wind dynamics evidenced in a multi-temporal study also showed that the near-absence of movement of this crest parallel to the beach line and the GPR also demonstrate that the wind corridors flow on bared stretches on the referred crest have been unable to form downstream dunes. On the other hand, the foredunes on the northeastern Brazilian coast likely have their internal limits acting as sediment suppliers to develop parabolic hairpin dunes. As the sediment bypasses them, or by blowout developed from the beach (Figure 8), sand is transported leeward of these foredunes to form parabolic, barchan and barchanoid dunes.

Therefore, this is another distinctive aspect of this ridge parallel to the beach, the adjacent foredunes, and other occurrences distributed along the coast of the State of Ceará. Therefore, the process of anthropic formation of this aeolian crest in a position disconnected from the natural pattern can be decisive in decontextualizing this feature in the foredune model.

Based on this coastal stretch and other occurrences along the Brazilian Northeast coast, the evolutionary dynamics of foredunes generally are not of great magnitude, generally not evolving beyond the incipient foredunes stage [2]. Preliminary observations indicate that the characteristics of the east to the resort area predominate in most occurrences of foredunes along the Brazilian Northeast coast.

6. Conclusions

The analyzed anthropic ridge parallel to the beach is linked to the effectiveness of exogenous vegetation in retaining the sediments carried by the wind. The GPR sections of the crest show mostly simple structures compatible with a kind of incipient protodune, and its morphology poorly resembles foredune. The analyses of this morphology show inconsistency between foredunes' morphological and cross-strata stages. In addition, the aeolian morphology generated by the placement of branches and tree trunks in the high tide stretch also develops features different from those of the natural process. In both cases, the spatial positioning of geomorphological evolution is unusual for foredunes in the region, resulting in classificatory inadequacy. This morphology differs from the foredunes distributed locally and regionally along the coast.

On the other hand, this anthropic ridge presents characteristics of retention or precipitation dunes on its leeward side. These types of aeolian deposition in the region also occur quite far from the beach line in transgressive dunes. Therefore, this aeolian feature is a dominantly anthropogenic expression directly resulting from the introduction of exogenous vegetation aligned parallel to the coastline, which reflects the absence of a programmatic method for foredune formation, and is thus an inadequate objective in terms of coast protection. Therefore, it results from an attempt to intercept wind transport, aiming at anthropogenic occupation.

In addition, the development of V-shaped crests oblique to the beach line and parallel to each other seems to be the pattern of the foredunes in the region. The development of ridges parallel to the beach line results from wave action on foredunes. In contrast, this kind of similar ridge located far from the beach line results from anthropogenic activity. Thus, this morphology presents some aspects that are not characteristic of the classification of foredunes and are not common among the dunes naturally formed in the region. Therefore, it demands adequate classification to emphasize its anthropogenic character.

More research focusing on the genetics and anthropogenic interference in foredunes is necessary and urgent. These studies can generate useful information for the planning and management of coastal areas, especially in a scenario of global climate change.

Author Contributions: Conceptualization: A.M.d.C.; Data collection and Methodology: A.M.d.C., S.B.L.J., L.M.E., F.G.d.C.G.; Writing—Original draft preparation and Visualization: A.M.d.C., V.C.-S., L.d.S.P., F.G.d.C.G.; Supervision: A.M.d.C., V.C.-S., L.d.S.P. All authors have read and agreed to the published version of the manuscript.

Funding: The study has been supported by the project, "Use of invasive and non-invasive methods in the characterization of foredunes on the coast of Ceará—UFC—FUNCAP/LABOMAR/UFC".

Data Availability Statement: Not applicable.

Acknowledgments: Thanks to FUNCAP for the DCR Grant (Claudino-Sales, V.) and IC-FUNCAP Research scholar-ship (Eduardo, L.M). Thanks to CNPq for the Research Productivity Fellowship (316941/2021-2, Pinheiro, L.S.) and CAPES for the Visiting Professor Fellow—CAPES PRINT Program (Finance Code 001 Pinheiro, L.S.)

Conflicts of Interest: The authors declare no conflict of interest.

References

1. Hesp, P.A. A review of biological and geomorphological processes involved in the initiation and development of incipient foredunes. *Proc. R. Soc. Edinburgh. Sect. B. Biol. Sci.* **1989**, *96*, 181–201. [CrossRef]
2. Hesp, P.A. Foredunes and blowouts: Initiation, geomorphology and dynamics. *Geomorphology* **2002**, *48*, 245–268. [CrossRef]
3. SEMA. Atualização do projeto de Zoneamento Ecológico-econômico da Zona Costeira do Estado do Ceará. *Secretaria Estadual do Meioambinete do Ceará*. 2022, 264p. Available online: https://www.sema.ce.gov.br/gerenciamento-costeiro/zoneamento-ecologico-economico-da-zona-costeira-zeec/documentos-previos-para-consulta-publica-do-zeec/ (accessed on 11 August 2022).
4. Silva, L.C.; Araújo, R.C.P.; Maia, L.P.; Cavalcante, M.D. Zoneamento ecológico- econômico da zona costeira do estado do Ceará. In *Zoneamento Ecológico- Econômico do Ceará—Zona Costeira Maria Dias Cavalcante*; Maia, L.P., de Castro MIranda, P.d.T., Eds.; SEMACE: Fortaleza, Brazil, 2006; Volume 1, pp. 93–101.
5. Hesp, P.A.; Dillemburg, S.R.; Barbosa, E.G.; Tomazelli, L.J.; Ayup-Zouain, R.N.; Esteves, L.S.; Gruber, N.L.S.; Toldo, E.E., Jr.; Tabajara, L.L.C.; Clerot, L.C.P. Beach ridges, foredunes or transgressive dunefields? Definitions and an examination of the Torres to Tramandaí barrier system, Southern Brazil. *An. Acad. Bras. Ciênc.* **2005**, *77*, 495–508. [CrossRef]
6. Hesp, P.A. The Beach Backshore and Beyond. In *Handbook of Beach and Shoreface Morphodynamics*; Short, A.D., Ed.; John Wiley and Sons: Chichester, UK, 1999; pp. 145–170.
7. Hesp, P.A.; Smyth, T.A.G. Anchored Dunes. In *Aeolian Geomorphology: A New Introduction*, 1st ed.; Livingstone, I., Warren, A., Eds.; Wiley-Blackwell: Hoboken, NJ, USA, 2019; pp. 157–178.
8. Cooper, W.S. Coastal sand dunes of Oregon and Washington. In *GSA Memoirs*; Geological Society of America: Boulder, CO, USA, 1958; Volume 72, pp. 1–162.
9. Olson, J.S.; van der Maarel, E. Coastal dunes in Europe: A global view. In *Perspectives in Coastal Dune Management*; Van der Meulen, F., Jungerius, P.D., Visser, J., Eds.; SPB Academic Publishing: The Hague, The Netherlands, 1989; pp. 1–32.
10. Godfrey, P.J. Climate, plant response, and development of dunes on barrier beaches along the US east coast. *Int. J. Biometeorol.* **1977**, *21*, 203–215. [CrossRef]
11. Goldsmith, V. Coastal sand dunes as geomorphological systems. *Proc. R. Soc. Edinb.* **1989**, *96B*, 3–15. [CrossRef]
12. Hemming, M.A.; Nieuwenhuize, J. Seagrass wrack-induced dune formation on a tropical coast (Banc d'Arguin, Mauritania). *Estuar. Coast. Shelf Sci.* **1990**, *31*, 499–502. [CrossRef]
13. Arens, S.M. Patterns of sand transport on vegetated foredunes. *Geomorphology* **1996**, *17*, 339–350. [CrossRef]
14. Eamer, J.B.R.; Walker, I.J. Quantifying sand storage capacity of large woody debris on beaches using LiDAR. *Geomorphology* **2010**, *118*, 33–47. [CrossRef]
15. Luna, M.C.M.; Parteli, E.J.R.; Duran, O.; Herrmann, H. Model for the genesis of coastal dune fields with vegetation. *Geomorphology* **2011**, *129*, 215–224. [CrossRef]
16. Bird, E.F.C. The Formation of Sand Beach-ridges. *Aust. J. Sci.* **1960**, *22*, 349–350.
17. Goldsmith, V. Internal geometry and origin of vegetated coastal sand dunes. *J. Sedim. Pet.* **1973**, *43*, 1128–1143.
18. Hesp, P.A. Foredune formation in Southeast Australia. In *Coastal Geomorphology in Australia*; Thom, B.G., Ed.; Academic Press: Cambridge, MA, USA, 1984; pp. 69–97.
19. Hesp, P.A. Morphology, dynamics and internal stratification of some established foredunes in southeast Australia. *Sediment. Geol.* **1988**, *55*, 17–41. [CrossRef]
20. Byrne, M.L.; McCann, S.B. Strati®cation and sedimentation in complex vegetated coastal dunes, Sable Island, Nova Scotia. *Sedim. Geol.* **1990**, *66*, 165–179. [CrossRef]
21. Hesp, P.A.; Smyth, T.A.G.; Nielsen, P.; Walker, I.J.; Bauer, B.O.; Davidson-Arnott, R.G. Flow deflection over a foredune. *Geomorphology* **2015**, *230*, 64–74. [CrossRef]
22. Arens, S.M.; Baas, A.C.W.; van Boxel, J.H.; Kalkman, C. Influence of reed stem density on foredune development. *Earth Surf. Process. Landf.* **2001**, *26*, 176. [CrossRef]

23. Davidson-Arnott, R.G.D.; Law, M.N. Seasonal patterns and controls on sediment supply to coastal foredunes, Long Point, Lake Erie. In *Coastal Dunes: Form and Process*; Nordstrom, K.F., Psuty, N.P., Carter, R.W.G., Eds.; Wiley: Hoboken, NJ, USA, 1990.
24. Kuriyama, Y.; Mochizuki, N.; Tsuyoshi, N. Inuence of vegetation on aeolian sand transport rate from a backshore to a foredune at Hasaki, Japan. *Sedimentology* **2005**, *52*, 1123–1132. [CrossRef]
25. McLean, R.; Shen, J.S. From foreshore to foredune: Foredune development over the last 30 years at Moruya Beach, New South Wales. *J. Coast. Res.* **2006**, *22*, 28–36. [CrossRef]
26. Zarnetske, P.L.; Ruggiero, P.; Seabloom, E.W.; Hacker, S.D. Coastal foredune evolution: The relative influence of vegetation and sand supply in the US Pacific Northwest. *J. R. Soc. Interface* **2015**, *12*, 20150017. [CrossRef]
27. De Vries, S.; Southgate, H.; Kanning, W.; Ranasinghe, R. Dune behavior and aeolian transport on decadal timescales. *Coast. Eng.* **2012**, *67*, 41–53. [CrossRef]
28. Durán, O.; Moore, L.J. Vegetation controls on the maximum size of coastal dunes. *Proc. Natl. Acad. Sci. USA* **2013**, *110*, 17217–17222. [CrossRef]
29. Keijsers, J.G.S.; De Groot, A.V.; Riksen, M.J.P.M. Vegetation and sedimentation on coastal foredunes. *Geomorphology* **2015**, *228*, 723–734. [CrossRef]
30. Houston, J.A.; Jones, C.R. The Sefton Coast management scheme: Project and process. *Coast. Manag.* **1987**, *15*, 267–297. [CrossRef]
31. Carlson, J.; Reckendorf, F.; Temyik, W. Stabilizing Coastal Sand Dunes in the Pacific Northwest. In *USDA Soil Conservation Service SCS Agriculture Handbook*; United States Department of Agriculture: Washington, DC, USA, 1991; Volume 687, 53p.
32. Arens, S.M.; Jungerius, P.D.; van der Meulen, F. Coastal dunes. In *Chapter 9: Habitat Conservation: Managing the Physical Environment*; Warren, A., French, J.R., Eds.; Wiley: New York, NY, USA, 2001.
33. Edmondson, S.E.; Velmans, C. Public perception of nature management on a sand dune system. In *Coastal Dune Management: Shared Experience of European Conservation Practice*; Houston, J.A., Edmondson, S.E., Rooney, P.J., Eds.; Liverpool University Press: Liverpool, UK, 2001; pp. 206–218.
34. Zwart, F. Dune management and communication with local inhabitants. In *Coastal Dune Management: Shared Experience of European Conservation Practice*; Houston, J.A., Edmondson, S.E., Rooney, P.J., Eds.; Liverpool University Press: Liverpool, UK, 2001; pp. 219–222.
35. Allan, J.C.; Komar, P.D.; Hart, R. A dynamic revetment and reinforced dune as "natural" forms of shore protection in an Oregon state park. In Proceedings of the Coastal Structures 2003 Conference, Portland, OR, USA, 26–30 August 2003; pp. 1048–1060.
36. Allan, J.C.; Komar, P.D. Environmentally compatible cobble berm and artificial dune for shore protection. *Shore Beach* **2004**, *72*, 9–18.
37. Komar, P.D.; Allan, J.C. "Design with Nature" Strategies for Shore Protection—The Construction of a Cobble Berm and Artificial Dune in an Oregon State Park: U.S. Geological Survey Scientific Investigations Report 2010, 2010–5254. Available online: https://pubs.usgs.gov/sir/2010/5254/pdf/sir20105254_chap12.pdf (accessed on 11 August 2022).
38. Nordstrom, K.F.; Jackson, N.L. Foredune Restoration in Urban Settings. In *Chapter 2: Restoration of Coastal Dunes*; Springer Series 17 on Environmental Management; Martínez, L.M., Gallego-Fernández, J.B., Hesp, P.A., Eds.; Springer: Berlin/Heidelberg, Germany, 2013. [CrossRef]
39. Portz, L.; Manzolli, R.P.; Hermanns, L.; Carrio, J.A. Evaluation of the efficiency of dune reconstruction techniques in Xangri-la (Rio Grande do Sul, Brazil). *Ocean. Coast. Manag.* **2015**, *104*, 78–89. [CrossRef]
40. Elko, N.; Brodie, K.; Stockdon, H.; Nordstrom, K.; Houser, C.; McKenna, K.; Moore, L.; Rosati, J.; Ruggiero, P.; Thuman, R.; et al. Dune management challenges on developed coasts. *Shore Beach* **2016**, *84*, 15.
41. Arens, S.M. Aeolian Processes in the Dutch Foredunes. Ph.D. Thesis, University of Amsterdam, Amsterdam, The Netherlands, 1994; 150p.
42. Arens, S.M.; van der Lee, G.E.M. Saltation sand traps for the measurement of aeolian transport into the foredunes. *Soil Technol.* **1995**, *8*, 61–74. [CrossRef]
43. Arens, S.M. Rates of aeolian sand transport on a beach in a temperate humid climate. *Geomorphology* **1996**, *17*, 3–18. [CrossRef]
44. Arens, S.M. Transport rates and volume changes in a coastal foredune on a Dutch Wadden island. *J. Coast. Conserv.* **1997**, *3*, 49–56. [CrossRef]
45. Matias, A.; Ferreira, O.; Mendes, I.; Dias, J.A.; Vila-Concejo, A. Artificial Construction of Dunes in the South of Portugal. *J. Coast. Res.* **2005**, *21*, 472–481. [CrossRef]
46. Eichmanns, C.; Schüttrumpf, H. Influence of Sand Trapping Fences on Dune Toe Growth and Its Relation with Potential Aeolian Sediment Transport. *J. Mar. Sci. Eng.* **2021**, *9*, 850. [CrossRef]
47. Eichmanns, C.; Lechthaler, S.; Zander, W.; Pérez, M.V.; Blum, H.; Thorenz, F.; Schüttrumpf, H. Sand Trapping Fences as a Nature-Based Solution for Coastal Protection: An International Review with a Focus on Installations in Germany. *Environments* **2021**, *8*, 135. [CrossRef]
48. Tsoar, H.; Levin, N.; Porat, N.; Maia, L.P.; Herrmann, H.J.; Tatumi, S.H.; Claudino-Sales, V. The effect of climate change on the mobility and stability of coastal sand dunes in Ceará State (NE Brazil). *Quat. Res.* **2009**, *71*, 217–226. [CrossRef]
49. Ferreira, A.G.; da Silva Mello, N.G. Principais Sistemas atmosféricos atuantes sobre a região Nordeste do Brasil e a influência dos oceanos Pacíficos e Atlântico no clima da região. *Rev. Bras. Climatol.* **2015**, *1*, 15–28. [CrossRef]
50. Claudino-Sales, V. Lagoa do Papipu: Natureza e Ambiente na Cidade de Fortaleza, Ceara. Master's Thesis, Universidade de Sao Paulo, Sao Paulo, Brazil, 1993.

51. Carvalho, A.M. Dinâmica Costeira entre Cumbuco e Matões-Costa NW do Estado do Ceará. Ênfase nos Processos Eólicos. Ph.D. Thesis, Universidade Federal da Bahia, Salvador, Brazil, 2003; 188p.
52. Pinheiro, L.; de Morais, J.O.; Maia, L.P. The Beaches of Ceará. In *Brazilian Beach Systems. Coastal Research Library*; Short, A., Klein, A., Eds.; Springer: Cham, Switzerland, 2016; Volume 17. [CrossRef]
53. Silvester, R. Growth of crenulate shaped bays to equilibrium. *J. Water Harb. Div. Am. Soc. Civ. Eng.* **1970**, *76*, 275–287. [CrossRef]
54. Hsü, J.R.-C.; Evans, C. Parabolic bay shapes and applications. In *Proceedings of Institution of Civil Engineers—Part 2*; Thomas Telford: London, UK, 1989.
55. Hsü, J.R.C.; Uda, T.; Silvester, R. Beach downcoast of harbours in bays. *Coast. Eng.* **1993**, *19*, 163–181. [CrossRef]
56. Carvalho, A.M.; Ellis, J.T.; Lamothe, M.; Maia, L.M. Using Wind Direction and Shoreline Morphology to Model Sand Dune Mobilization. *J. Coast. Res.* **2016**, *32*, 1005–1015. [CrossRef]
57. Miot da Silva, G.; Hesp, P.A. Coastline orientation, aeolian sediment transport and foredune and dunefield dynamics of Moçambique Beach, Southern Brazil. *Geomorphology* **2010**, *120*, 258–278. [CrossRef]
58. Annan, A.P. *Ground Penetration Radar*; Internal Report; Workshop Notes, Sensors and Software, Inc.: Mississauga, ON, Canada, 1992; 130p.
59. Daniels, J.J. Fundamentals of ground penetrating radar. In Proceedings of the Symposium on the Application of Geophysics to Engineering and Environmental Problems, Golden, CO, USA, 13–16 March 1989; pp. 62–142.
60. Annan, A.P. Pratical processing of GPR data. In Proceedings of the Second Government Workshop on Ground Penetrating Radar, Columbus, OH, USA, 26–28 October 1993; Volume 2.
61. Suguio, K. *Introdução à Sedimentologia*; EDUSP: São Paulo, SP, USA, 1973; 317p.
62. Wentworth, C.K. A scale of grade and class terms for clastic sediments. *J. Geol.* **1922**, *30*, 377–392. [CrossRef]
63. De Camargo, M.G. Sysgran: Um sistema de código aberto para análises granulométricas do sedimento. *Rev. Bras. Geociênc.* **2006**, *36*, 371–378. [CrossRef]
64. Folk, R.L.; Ward, W.C. Brazos River bar: A study in the significance of grain size parameters. *J. Sediment. Petrol.* **1957**, *27*, 3–26. [CrossRef]
65. Anders, F.; Leatherman, S. Disturbance of beach sediment by off-road vehicles. *Environ. Geol.* **1987**, *9*, 183–189. [CrossRef]
66. Anders, F.J.; Leatherman, S.P. Effects of off-road vehicles on coastal foredunes at Fire Island, New York, USA. *Environ. Manag.* **1987**, *11*, 45–52. [CrossRef]
67. Bruun, P. Beach scraping—Is it damaging to beach stability? *Coast. Eng.* **1983**, *7*, 167–173. [CrossRef]
68. Smyth, T.A.G.; Hesp, P.A. Aeolian dynamics of beach scraped ridge and dyke structures. *Coast. Eng.* **2015**, *99*, 38–45. [CrossRef]
69. Cooper, W.S. Coastal dunes of California. In *GSA Memoirs*; Geological Society of America: Boulder, CO, USA, 1967; Volume 104, pp. 1–124.
70. Hesp, P.A. Dune Coasts. In *Treatise on Estuarine and Coastal Science*; Wolanski, E., McLusky, D.S., Eds.; Academic Press: Waltham, MA, USA, 2011; Volume 3, pp. 193–221.
71. Melton, F.A. A tentative classification of sand dunes its application to dune history in the southern High Plains. *Geology* **1940**, *48*, 113–174. [CrossRef]
72. Marston, R.A. Maneuver-caused wind erosion impacts, south central New Mexico. In *Aeolian Geomorphology*; Nickling, W.G., Ed.; Allen and Unwin: Boston, MA, USA, 1986; pp. 273–290.
73. Khalaf, F.I.; Misak, R.; Al-Dousari, A. Sedimentological and morphological characteristics of some nabkha deposits in the northern coastal plain of Kuwait, Arabia. *J. Arid. Environ.* **1995**, *29*, 267–292. [CrossRef]
74. Carter, R.W.G.; Hesp, P.A.; Nordstrom, K.F. Erosional landforms in coastal dunes. In *Coastal Dunes: Form and Process*; Nordstrom, K.F., Psuty, N.P., Carter, R.W.G., Eds.; Wiley: Chichester, UK, 1990; pp. 217–249.
75. Jackson, D.W.T.; Beyers, M.; Delgado-Fernandez, I.; Baas, A.C.W.; Cooper, A.J.; Lynch, K. Airflow reversal and alternating corkscrew vortices in foredune wake zones during perpendicular and oblique offshore winds. *Geomorphology* **2013**, *187*, 86–93. [CrossRef]
76. Bauer, B.O.; Davidson-Arnott, R.G.D.; Walker, I.J.; Hesp, P.A.; Ollerhead, J. Wind direction and complex sediment transport response across a beach-dune system. *Earth Surf. Process. Landf.* **2012**, *37*, 1661–1677. [CrossRef]
77. Bauer, B.O.; Walker, I.J.; Baas, A.C.W.; Jackson, D.W.T.; Neuman, C.M.; Wiggs, G.F.S.; Hesp, P.A. Critical reflections on the coherent flow structures paradigm in aeolian geomorphology. In *Coherent Flow Structures at Earth's Surface*; Venditti, J.G., Best, J.L., Church, M., Hardy, R.J., Eds.; John Wiley: Chichester, UK, 2013; pp. 111–134. [CrossRef]
78. Schwarz, C.; van Starrenburg, C.; Donker, J.; Ruessink, G. Wind and sand transport across a vegetated foredune slope. *J. Geophys. Res. Earth Surf.* **2020**, *125*, e2020JF005732. [CrossRef]
79. Bauer, B.O.; Davidson-Arnott, R.G.D. A general framework for modeling sediment supply to coastal dunes including wind angle, beach geometry, and fetch effects. *Geomorphology* **2003**, *49*, 89–108. [CrossRef]
80. Carvalho, A.M.; Lima, S.B., Jr.; Maia, L.P.; Claudino-Sales, V.; Gastão, F.G.C.; Eduardo, L.M.; Pinheiro, L.S.; Silva, M.V.C. Understanding polydirectional aeolian cross-strata architecture in a coastal unidirectional wind regime. *J. Coast. Res.* **2021**, *37*, 364–379, Coconut Creek (Florida). [CrossRef]
81. Cooper, A.; Jackson, D. Dune gardening? A critical view of the contemporary coastal dune management paradigm. *Area* **2021**, *53*, 345–352. [CrossRef]

82. Van der Wal, D. *Aeolian Transport of Nourishment Sand in Beach-Dune Environments*; Universiteit van Amsterdam: Amsterdam, The Netherlands, 1999.
83. Saunders, K.E.; Davidson-Arnott, R.G.D. Coastal dune response to natural disturbances. In Proceedings of the Symposium on Coastal Sand Dunes 1990, Guelph, ON, Canada, 12–14 September 1990; National Research Council: Ottawa, ON, Canada, 1990; pp. 321–345.
84. Zarnetske, P.L.; Hacker, S.D.; Seabloom, E.W.; Ruggiero, P.; Killian, J.R.; Maddux, T.B.; Cox, D. Biophysical feedback mediates eects of invasive grasses on coastal dune shape. *Ecology* **2012**, *93*, 1439–1450. [CrossRef] [PubMed]
85. Nordstrom, K.F. Beaches and dunes of human-altered coasts. *Prog. Phys. Geogr.* **1994**, *18*, 497–516. [CrossRef]
86. Dugan, J.E.; Hubbard, D.M.; Rodil, I.F.; Revell, D.L.; Schroeter, S. Ecological effects of coastal armoring on sandy beaches. *Mar. Ecol.* **2008**, *29* (Suppl. 1), 160–170. [CrossRef]
87. Bressolier, C.; Thomas, Y.-F. Studies on wind and plant interactions on French Atlantic coastal dunes. *J. Sediment. Petrol.* **1977**, *47*, 331–338.
88. Hesp, P.A. The formation of shadow dunes. *J. Sediment. Petrol.* **1981**, *51*, 101–112.
89. Nickling, W.G.; Davidson-Arnott, R.G.D. Aeolian sediment transport on beaches and coastal dunes. In Proceedings of the Symposium on Coastal Sand Dunes 1990, Guelph, ON, Canada, 12–14 September 1990; National Research Council: Ottawa, ON, Canada, 1990; pp. 1–35.
90. Pye, K.; Tsoar, H. *Aeolian Sand and Sand Dunes*; Unwin Hyman: London, UK, 1990; p. 396.
91. Ahlbrandt, T.S.; Swinehart, J.B.; Maroney, D.G. The dynamic Holocene dune fields of the Great Plains and Rocky Mountain basins, U.S.A. In *Eolian Sediments*; Brookfield, M.E., Ahlbrandt, T.S., Eds.; Elsevier: Amsterdam, The Netherlands, 1983; Volume 38, pp. 379–406.
92. Tinley, K.L. *Coastal dunes of South Africa, South African National Scientific Programmes Report*; Council for Scientific and Industrial Research: Pretoria, South Africa, 1985; Volume 109, 300p.
93. Holm, D.A. Desert geomorphology in the Arabian Peninsula. *Science* **1960**, *132*, 1369–1379. [CrossRef]
94. Warren, A. Dunes in the Tenere desert. *Geogr. J.* **1971**, *137*, 458–461. [CrossRef]
95. Wilson, I.G. Ergs. *Sediment. Geol.* **1973**, *10*, 77–106. [CrossRef]
96. Nielson, J.; Kocurek, G. Climbing zibars of the Algodones. *Sed. Geol.* **1986**, *48*, 1–15. [CrossRef]
97. Kocurek, G.; Townsley, M.; Yeh, E.; Havholm, K.; Sweet, M.L. Dune and dune-field development on Padre Island, Texas, with implications for interdune deposition and water-table-controlled accumulation. *J. Sediment. Res.* **1992**, *62*, 622–635.
98. Lancaster, N. Dunes on the Skeleton Coast, Namibia (South West Africa): Geomorphology and grain size relationships. *Earth Surf. Proc. Land* **1982**, *7*, 575–587. [CrossRef]
99. Lancaster, N. Field studies of sand patch initiation processes on the northern margin of the Namib sand sea. *Earth Surf. Proc. Land* **1996**, *21*, 947–954. [CrossRef]
100. Kroy, K.; Sauermann, G.; Herrmann, H.J. Minimal model for sand dunes. *Phys. Rev. Lett.* **2002**, *88*, 054301. [CrossRef] [PubMed]
101. Momiji, H.; Nishimori, H.; Bishop, S.R. On the shape and migration speed of a proto-dune. *Earth Surf. Proc. Land* **2002**, *27*, 1335–1338. [CrossRef]
102. Elbelrhiti, H.; Claudin, P.; Andreotti, B. Field evidence for surface-wave-induced instability of sand dunes. *Nature* **2005**, *437*, 720. [CrossRef]
103. Bristow, C.S.; Jol, H.M.; Augustinus, P.; Wallis, I. Slipfaceless 'whaleback' dunes in a polar desert, Victoria Valley, Antarctica: Insights from ground penetrating radar. *Geomorphology* **2010**, *114*, 361–372. [CrossRef]
104. Andreotti, B.; Claudin, P.; Pouliquen, O. Measurements of the aeolian sand transport saturation length. *Geomorphology* **2010**, *123*, 343–348. [CrossRef]
105. Elbelrhiti, H. Initiation and early development of barchan dunes: A case study of the Moroccan Atlantic Sahara desert. *Geomorphology* **2012**, *138*, 181–188. [CrossRef]
106. Nield, J.M.; Wiggs, G.F.; Squirrell, R.S. Aeolian sand strip mobility and protodune development on a drying beach: Examining surface moisture and surface roughness patterns measured by terrestrial laser scanning. *Earth Surf. Proc. Land* **2011**, *36*, 513–522. [CrossRef]
107. Ewing, R.C.; McDonald, G.D.; Hayes, A.G. Multi-spatial analysis of aeolian dune field patterns. *Geomorphology* **2015**, *240*, 44–53. [CrossRef]
108. Kocurek, G.; Ewing, R.C. Trickle-Down and trickle-up boundary conditions in eolian dune-field pattern formation. In *Autogenic Dynamics and Self-Organization in Sedimentary Systems*; Budd, D.A., Hajek, E.A., Purkis, S.J., Eds.; SEPM (Society for Sedimentary Geology): Tulsa, OK, USA, 2016; pp. 5–17. [CrossRef]
109. Phillips, J.D.; Ewing, R.C.; Bowlinga, R.R.; Weymerb, B.A.; Barrineauc, P.; Nittrouerd, J.A.; Everetta, M.E. Low-angle eolian deposits formed by protodune migration, and insights into slipface development at White Sands Dune Field, New Mexico. *Aeolian Res.* **2019**, *36*, 9–26. [CrossRef]
110. Goldsmith, V. Coastal dunes. In *Coastal Sedimentary Environments*; Davis, R.A., Ed.; Springer: New York, NY, USA, 1978; pp. 171–235.
111. Nordstrom, K.F.; Arens, S.M. The role of human actions in evolution and management of foredunes in The Netherlands and New Jersey, USA. *J. Coast. Conserv.* **1998**, *4*, 169–180. [CrossRef]